Essential role of the cytochrome P450 CYP4F22 in the production of acylceramide, the key lipid for skin permeability barrier formation

Yusuke Ohno[a], Shota Nakamichi[a], Aya Ohkuni[a], Nozomi Kamiyama[a], Ayano Naoe[b], Hisashi Tsujimura[b], Urara Yokose[b], Kazumitsu Sugiura[c], Junko Ishikawa[b], Masashi Akiyama[c], and Akio Kihara[a,1]

[a]Laboratory of Biochemistry, Faculty of Pharmaceutical Sciences, Hokkaido University, Kita-ku, Sapporo 060-0812, Japan; [b]Kao Corporation, Haga-gun, Tochigi 321-3497, Japan; and [c]Department of Dermatology, Nagoya University Graduate School of Medicine, Showa-ku, Nagoya 466-8550, Japan

Edited by David W. Russell, University of Texas Southwestern Medical Center, Dallas, TX, and approved May 21, 2015 (received for review February 19, 2015)

A skin permeability barrier is essential for terrestrial animals, and its impairment causes several cutaneous disorders such as ichthyosis and atopic dermatitis. Although acylceramide is an important lipid for the skin permeability barrier, details of its production have yet to be determined, leaving the molecular mechanism of skin permeability barrier formation unclear. Here we identified the cytochrome P450 gene *CYP4F22* (cytochrome P450, family 4, subfamily F, polypeptide 22) as the long-sought fatty acid ω-hydroxylase gene required for acylceramide production. *CYP4F22* has been identified as one of the autosomal recessive congenital ichthyosis-causative genes. Ichthyosis-mutant proteins exhibited reduced enzyme activity, indicating correlation between activity and pathology. Furthermore, lipid analysis of a patient with ichthyosis showed a drastic decrease in acylceramide production. We determined that CYP4F22 was a type I membrane protein that locates in the endoplasmic reticulum (ER), suggesting that the ω-hydroxylation occurs on the cytoplasmic side of the ER. The preferred substrate of the CYP4F22 was fatty acids with a carbon chain length of 28 or more (≥C28). In conclusion, our findings demonstrate that CYP4F22 is an ultra-long-chain fatty acid ω-hydroxylase responsible for acylceramide production and provide important insights into the molecular mechanisms of skin permeability barrier formation. Furthermore, based on the results obtained here, we proposed a detailed reaction series for acylceramide production.

acylceramide | ceramide | lipid | skin | sphingolipid

A skin permeability barrier protects terrestrial animals from water loss from inside the body, penetration of external soluble materials, and infection by pathogenetic organisms. In the stratum corneum, the outermost cell layer of the epidermis, multiple lipid layers (lipid lamellae) play a pivotal function in barrier formation (Fig. S1) (1–3). Impairment of the skin permeability barrier leads to several cutaneous disorders, such as ichthyosis, atopic dermatitis, and infectious diseases.

The major components of the lipid lamellae are ceramide (the sphingolipid backbone), cholesterol, and free fatty acid (FA). In most tissues, ceramide consists of a long-chain base (LCB; usually sphingosine) and an amide-linked FA with a chain length of 16–24 (C16–C24) (4, 5). On the other hand, ceramide species in the epidermis are strikingly unique (Fig. S2*A*). For example, epidermal ceramides contain specialized LCBs (phytosphingosine and 6-hydroxysphingosine) and/or FAs with α- or ω-hydroxylation (1–3). In addition, substantial amounts of epidermal ceramides have ultra-long-chain FAs (ULCFAs) with chain lengths of 26 or more (≥C26) (4, 5). Unique epidermal ceramides are acylceramides having C28–C36 ULCFAs, which are ω-hydroxylated and esterified with linoleic acid [EOS in Fig. S1; EODS, EOS, EOP, and EOH in Fig. S2*A*; EOS stands for a combination of an esterified ω-hydroxy FA (EO) and sphingosine (S); DS, dihydrosphingosine; P, phytosphingosine; H, 6-hydroxysphingosine] (1–3, 6, 7). These characteristic molecules may be important to increase the hydrophobicity of lipid lamellae and/or to stabilize the multiple lipid layers. Linoleic acid is one of the essential FAs, and its deficiency causes ichthyosis symptoms resulting from a failure to form normal acylceramide (8). Ichthyosis is a cutaneous disorder accompanied by dry, thickened, and scaly skin; it is caused by a barrier abnormality. In patients who have atopic dermatitis, both total ceramide levels and the chain length of ceramides are decreased, and ceramide composition is altered also (9–11).

In addition to its essential function in the formation of lipid lamellae, acylceramide also is important as a precursor of protein-bound ceramide, which functions to connect lipid lamellae and corneocytes (Fig. S1) (12, 13). After the removal of linoleic acid, the exposed ω-hydroxyl group of acylceramide is covalently bound to corneocyte proteins, forming a corneocyte lipid envelope. Acylceramides and protein-bound ceramides are important in epidermal barrier formation, and mutations in the genes involved in their synthesis, including the ceramide synthase *CERS3*, the 12(*R*)-lipoxygenase *ALOX12B*, and the epidermal lipoxygenase-3 *ALOXE3*, can cause nonsyndromic, autosomal recessive congenital ichthyosis (ARCI) (3, 14–16). CERS3 catalyzes the amide bond formation between an LCB and ULCFA, producing ULC-ceramide, which is the precursor of acylceramide (Fig. S1 and Fig. S2*B*) (17). ALOX12B and ALOXE3 are required for the formation of protein-bound ceramides (13, 18). Other ARCI genes include the ATP-binding cassette (ABC) transporter *ABCA12*, the transglutaminase *TGM1*, *NIPAL4* (NIPA-like domain containing

Significance

The sphingolipid backbone ceramide is the major lipid species in the stratum corneum and plays a pivotal function in skin permeability barrier formation. Acylceramide is an important epidermis-specific ceramide species. However, the details of acylceramide production, including its synthetic genes, reactions and their orders, and intracellular site for production, have remained unclear. In the present study, we identified the cytochrome P450, family 4, subfamily F, polypeptide 22 (CYP4F22) as the missing fatty acid ω-hydroxylase required for acylceramide synthesis. We also determined that CYP4F22 is a type I endoplasmic reticulum membrane protein and that its substrate is ultra-long-chain fatty acids. Our findings provide important insights into the molecular mechanisms of not only acylceramide production but also skin permeability barrier formation.

Author contributions: A.K. planned the project; Y.O. and A.K. designed research; K.S. and M.A. prepared stratum corneum samples; Y.O., S.N., A.O., and N.K. performed research; A.N., H.T., U.Y., and J.I. analyzed ceramide compositions; Y.O. analyzed data; and A.K. wrote the paper.

The authors declare no conflict of interest.

This article is a PNAS Direct Submission.

[1]To whom correspondence should be addressed. Email: kihara@pharm.hokudai.ac.jp.

This article contains supporting information online at www.pnas.org/lookup/suppl/doi:10.1073/pnas.1503491112/-/DCSupplemental.

4)/*ICHTHYIN*, *CYP4F22*/*FLJ39501*, *LIPN* (lipase, family member N), and *PNPLA1* (patatin-like phospholipase domain containing 1) (16, 19). The exact functions of *NIPAL4*, *LIPN*, and *PNPLA1* are currently unclear. Causative genes of syndromic forms of ichthyosis also include a gene required for acylceramide synthesis: the FA elongase *ELOVL4*, which produces ULCFA-CoAs, the substrate of CERS3 (20).

Although acylceramide is essential for the epidermal barrier function, the mechanism behind acylceramide production is still poorly understood, leaving the molecular mechanisms behind epidermal barrier formation unclear. For example, acylceramide production requires ω-hydroxylation of the FA moiety of ceramide. However, the ω-hydroxylase responsible for this reaction was unidentified heretofore (Fig. S1). Here, we identified the cytochrome P450, family 4, subfamily F, polypeptide 22 (CYP4F22), also known as "FLJ39501," as this missing FA ω-hydroxylase required for acylceramide production. *CYP4F22* had been identified as one of the ARCI genes (21), although its function in epidermal barrier formation remained unsolved. Our findings clearly demonstrate a relationship between ARCI pathology, acylceramide levels, and ω-hydroxylase activity.

Results

Identification of CYP4F22 as the FA ω-Hydroxylase Required for ω-Hydroxyceramide Production. Although researchers have long known that ω-hydroxylation is essential for acylceramide formation, they have puzzled over which gene is responsible for this reaction. To identify this gene, we first established a cell system that produced ULC-ceramides, a possible substrate of interest for ω-hydroxylase, because most cells cannot produce such extremely long ceramides. HEK 293T cells overproducing the FA elongase ELOVL4 and/or the ceramide synthase CERS3 were labeled with [^{3}H]sphingosine, and the chain lengths of ceramides were determined by reverse-phase TLC. Although overexpression of either ELOVL4 or CERS3 alone did not result in the production of ULC-ceramides, their co-overproduction caused generation of ULC-ceramides with ≥C26 (Fig. 1*A*). They migrated more slowly than long-chain (LC; C16–C20) ceramides and very long-chain (VLC; C22–C24) ceramides on reverse-phase TLC. Production of ULC-ceramides with chain lengths up to C36 also was confirmed by LC-MS analysis (Fig. S3). When labeled lipids were separated by normal-phase TLC, ULC-ceramides were detected as a band at the adjacent, upper position of VLC-ceramides (Fig. 1*B*).

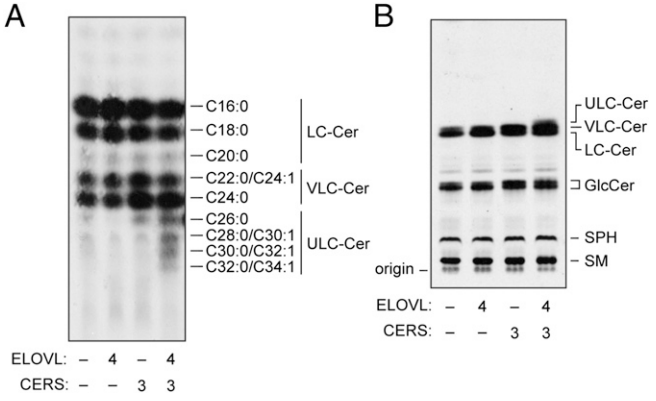

Fig. 1. Overproduction of ELOVL4 and CERS3 causes generation of ULC-ceramides. HEK 293T cells were transfected with plasmids encoding *3xFLAG-ELOVL4* and *3xFLAG-CERS3*, as indicated. Cells were labeled with [^{3}H]sphingosine for 4 h at 37 °C. Lipids were extracted, separated by reverse-phase TLC (*A*) or normal-phase TLC (*B*), and detected by autoradiography. Cer, ceramide; GlcCer, glucosylceramide; SM, sphingomyelin; SPH, sphingosine.

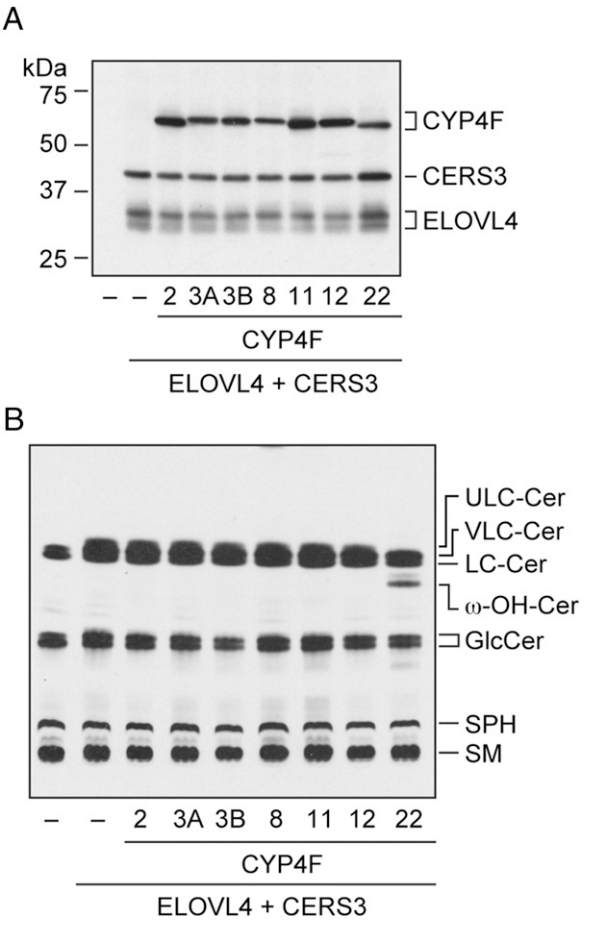

Fig. 2. CYP4F22 is involved in ω-hydroxyceramide synthesis. HEK 293T cells were transfected with plasmids encoding *3xFLAG-ELOVL4*, *3xFLAG-CERS3*, and *3xFLAG-CYP4F* subfamily members, as indicated. (*A*) Total lysates prepared from the transfected cells were separated by SDS/PAGE, followed by immunoblotting with anti-FLAG antibodies. (*B*) Cells were labeled with [^{3}H]sphingosine for 4 h at 37 °C. Lipids were extracted, separated by normal-phase TLC, and detected by autoradiography. Cer, ceramide; GlcCer, glucosylceramide; SM, sphingomyelin; SPH, sphingosine; ω-OH, ω-hydroxy.

It has been reported that the cytochrome P450 (CYP) inhibitor aminobenzotriazole inhibits the generation of ω-hydroxyceramide in cultured human keratinocytes (22). In humans, 57 *CYP* genes exist, and mammalian *CYP* genes are classified into 18 families and 43 subfamilies. Some CYP4F members are implicated in the ω-hydroxylation of long-chain FAs (23, 24), raising the possibility that certain CYP4F subfamily members are responsible for ω-hydroxylation of ULCFAs in acylceramide formation. To test this possibility, we cloned all the human *CYP4F* subfamily genes (*CYP4F2*, *3A*, *3B*, *8*, *11*, *12*, and *22*), and each was expressed as an N-terminally 3xFLAG-tagged protein in HEK 293T cells overproducing 3xFLAG-ELOVL4 and 3xFLAG-CERS3. All CYP4F subfamily proteins were expressed at similar levels (Fig. 2*A*). Among the CYP4F subfamily members, only CYP4F22 caused the disappearance of ULC-ceramide, which was concomitant with the production of a new band at the position of ω-hydroxyceramide (Fig. 2*B* and Fig. S4). LC-MS analysis determined that this band indeed represented ω-hydroxyceramides with C28–C36 (Fig. S5). Thus, CYP4F22 is the ω-hydroxylase required for ω-hydroxyceramide production.

Correlation Between CYP4F22 Activity and Ichthyosis Pathology. Although the *CYP4F22* gene has been identified as one of the

ARCI-causative genes (21, 25), its function in epidermal barrier formation has remained unsolved. Five missense mutations, all of which cause amino acid substitutions (F59L, R243H, R372W, H435Y, and H436D), have been found in the *CYP4F22* of patients with ichthyosis. To examine their role in ichthyosis pathology, we introduced these mutations into *CYP4F22* and examined the ω-hydroxylase activity of the resultant mutant proteins. All mutant proteins were expressed at levels equivalent to the wild-type protein (Fig. 3*A*), and indeed all ω-hydroxylase activity of the mutant CYP4F22 proteins decreased to 4–20% of wild-type protein activity (Fig. 3*B*). Therefore, protein activity and ichthyosis pathology were nicely correlated.

Those points being noted, ichthyosis resulting from *CYP4F22* mutation is quite rare. In fact, only ∼20 patients have been reported in Mediterranean populations (21), and only a single patient has been reported in Japan (25). The Japanese patient has compound heterozygous *CYP4F22* mutations: One is a point mutation (c.728G→A) causing an amino acid substitution (p.R243H; R243H), and the other is a deletion (c.1138delG) causing a frame shift (p.D380TfsX2; D380TfsX2) in which Asp380 is replaced by Thr followed by a stop codon (25). The mutant R243H exhibited decreased activity as described above (Fig. 3*B*). We also introduced the c.1138delG mutation into *CYP4F22* and examined the ω-hydroxylase activity of its truncated protein product. D380TfsX2 (predicted molecular mass, 44.8 kDa) migrated faster than the wild-type protein (62.0 kDa; Fig. 3*A*), and we found that it exhibited no activity (Fig. 3*B*).

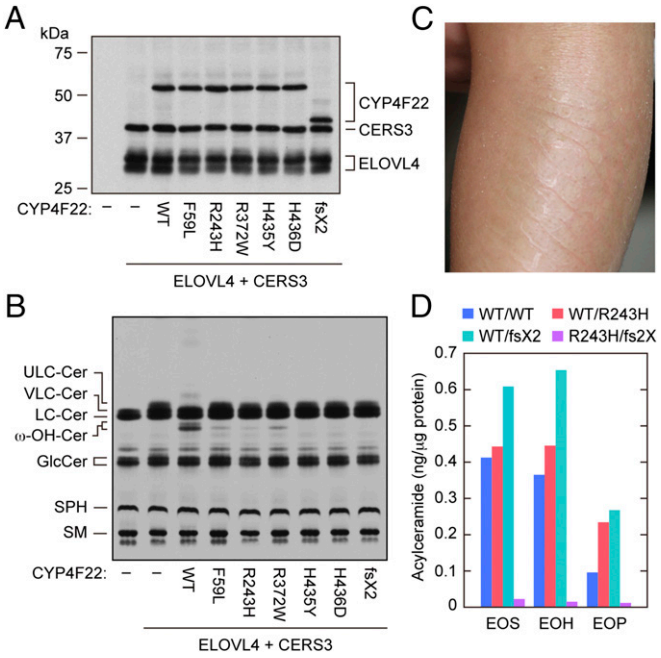

Fig. 3. Hydroxylase activity of CYP4F22 is impaired by ichthyosis-causing mutations. (*A* and *B*) HEK 293T cells were transfected with plasmids encoding *3xFLAG-ELOVL4*, *3xFLAG-CERS3*, and *3xFLAG-CYP4F22* (wild type or mutant), as indicated. (*A*) Total cell lysates prepared from the transfected cells were separated by SDS/PAGE and subjected to immunoblotting with anti-FLAG antibodies. (*B*) The transfected cells were labeled with [^{3}H]sphingosine for 4 h at 37 °C. Extracted lipids were separated by normal-phase TLC and detected by autoradiography. Cer, ceramide; GlcCer, glucosylceramide; SM, sphingomyelin; SPH, sphingosine; ω-OH, ω-hydroxy. (*C*) Representative clinical feature of a 2-y-old ARCI patient. Leaf-like flakes presented on the extensor side of the left lower limb before tape stripping. (*D*) Acylceramide (EOS, EOH, and EOP) levels in stratum corneum of a control (WT/WT), carriers (WT/R243H, the ichthyosis patient's father, and WT/D380T fs2X (fs2X), the patient's mother), and an ARCI patient (R243H/D380T fs2X) were measured by LC-MS.

To confirm our conclusion that CYP4F22 is involved in the production of acylceramide through ω-hydroxyceramide synthesis, we subjected the stratum corneum of the Japanese patient (Fig. 3*C*) and those of controls (her parents and a healthy volunteer) to LC-MS analysis and examined the levels of 11 major ceramide species. Although statistical analysis could not be performed because of the low number of samples, all three acylceramides containing sphingosine (EOS), 6-hydroxysphingsoine (EOH), and phytosphingosine (EOP) were apparently decreased in the ARCI patient to one tenth of the levels in controls (Fig. 3*D* and Table S1). Instead, the nonacylated ceramides NS (which is a combination of sphingosine and a nonhydroxylated FA) and AS (which is a combination of sphingosine and an α-hydroxylated FA) seemed to be increased (Table S1). These results confirm that ω-hydroxyceramide production by CYP4F22 is indeed required for acylceramide synthesis.

CYP4F22 Is a Type I Endoplasmic Reticulum Membrane Protein. We next examined the subcellular localization of CYP4F22 by subjecting 3xFLAG-tagged CYP4F22 to indirect immunofluorescence microscopy (Fig. 4*A*). 3xFLAG-CYP4F22 exhibited a reticular localization pattern and was colocalized with calnexin, HA-ELOVL4, and HA-CERS3, all of which are endoplasmic reticulum (ER) proteins, indicating that CYP4F22 is localized in the ER. A hydropathy plot showed that CYP4F22 contains a highly hydrophobic region at the N terminus as well as some weak hydrophobic stretches (Fig. 4*B*). To reveal the membrane topology of CYP4F22, we introduced an N-glycosylation cassette, which is N-glycosylated when exposed to the lumen of the ER, into several positions of CYP4F22: the N terminus, E85/K (between Glu85 and Lys86 residues), H155/R, A285/L, C361/R, D455/N, and R508/K. Of these fusion proteins, only CYP4F22 containing the N-glycosylation cassette at the N terminus received glycosylation, because the shift in molecular weight was observed upon treatment with endoglycosidase H (Fig. 4*C*). This result indicates that CYP4F22 spans the ER membrane once. Furthermore, it oriented its N terminus to the ER lumen and oriented the large, hydrophilic C-terminal domain containing the active site to the cytosolic side of the ER membrane. The same membrane topology was determined for other CYP members by the detection of N-terminal N-glycosylation (26, 27).

When the N-terminal hydrophobic region was removed, the resulting CYP4F22ΔN became distributed throughout the cytoplasm (Fig. 4*D*). CYP4F22ΔN was fractionated into both soluble and membrane fractions by ultracentrifugation, in contrast to full-length CYP4F22, which was detected only in the membrane fraction (Fig. 4*E*). These results confirmed that CYP4F22 is a type I ER membrane protein. CYP4F22ΔN could not produce ω-hydroxyceramide (Fig. 4*F*), suggesting that anchoring to the ER membrane, where all the reactions of acylceramide synthesis occur, is crucial for the CYP4F22 function.

ULCFAs Are Substrates of CYP4F22. It was still unclear whether CYP4F22 introduces an ω-hydroxyl group into ULCFAs before or after the formation of ceramide. Therefore, we examined ω-hydroxy FA levels using LC-MS in the presence of the ceramide synthase inhibitor fumonisin B_1. If ω-hydroxylation occurs before ceramide production, it was expected that free ω-hydroxy FA levels should be increased with fumonisin B_1 treatment. We found that ω-hydroxy FA levels with C26–C36 were increased significantly by the addition of fumonisin B_1 (Fig. 5*A*), suggesting that ω-hydroxylation occurs before ceramide production. Thus, it is highly likely that the substrates of CYP4F22 are not ceramides but rather are FAs, the same type of substrate catalyzed by other CYP4F family members.

To confirm that the substrates of CYP4F22 are FAs, we performed an in vitro analysis using yeast, which has no endogenous FA ω-hydroxylase activity. When C30:0 FA was used as a substrate,

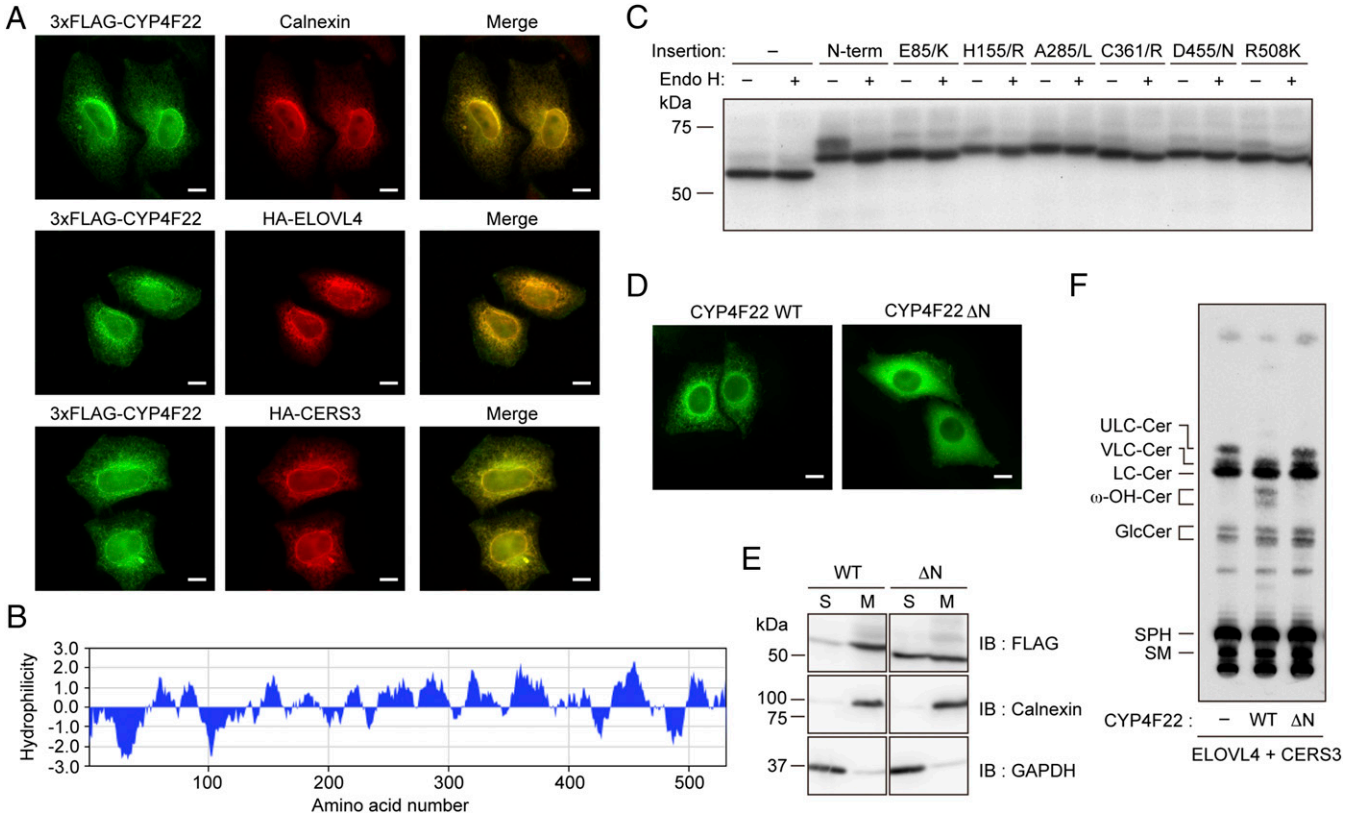

Fig. 4. CYP4F22 is a type I ER membrane protein. (*A*, *D*, and *E*) HeLa cells were transfected with plasmids encoding *HA-ELOVL4*, *HA-CERS3*, *3xFLAG-CYP4F22*, and *3xFLAG-CYP4F22ΔN* (CYP4F22 lacking 54 N-terminal amino acids), as indicated. (*A* and *D*) Cells were subjected to indirect immunofluorescence microscopic observation. (Scale bars, 10 μm.) (*B*) The hydrophilicity of CYP4F22 was analyzed by MacVector software (MacVector) using the Kyte and Doolittle algorithm (window size, 15). (*C*) HEK 293T cells were transfected with pCE-puro 3xFLAG-CYP4F22, pCE-puro 3xFLAG-CYP4F22 (N-term: insertion of the N-glycosylation cassette to the N terminus), pCE-puro 3xFLAG-CYP4F22 (E85/K: insertion of the cassette between Glu-85 and Lys-86), pCE-puro 3xFLAG-CYP4F22 (H155/R), pCE-puro 3xFLAG-CYP4F22 (A285/L), pCE-puro 3xFLAG-CYP4F22 (C361/R), pCE-puro 3xFLAG-CYP4F22 (D455/N), or pCE-puro 3xFLAG-CYP4F22 (R508/K). Lysates (3 μg) prepared from transfected cells were treated with or without endoglycosidase H (Endo H) and were separated by SDS/PAGE, followed by immunoblotting with anti-FLAG antibodies. (*E*) Total cell lysates (10 μg) were centrifuged at 100,000 × *g* for 30 min at 4 °C. The resulting supernatant (soluble fraction, S) and pellet (membrane fraction, M) were subjected to immunoblotting using anti-FLAG, anti-calnexin (membrane protein marker) or anti-GAPDH (soluble protein marker) antibodies. IB, immunoblotting. (*F*) HEK 293T cells transfected with plasmids encoding *3xFLAG-ELOVL4*, *3xFLAG-CERS3*, and *3xFLAG-CYP4F22* [wild type or *CYP4F22ΔN* (ΔN)], as indicated, were labeled with [^{3}H]sphingosine for 4 h at 37 °C. Lipids were extracted, separated by normal-phase TLC, and detected by autoradiography. Cer, ceramide; GlcCer, glucosylceramide; SM, sphingomyelin; SPH, sphingosine; ω-OH, ω-hydroxy.

the total membrane fractions prepared from yeast bearing a vector plasmid exhibited FA ω-hydroxylase activity only at background levels (Fig. 5*B*). On the other hand, the ectopic expression of human CYP4F22 resulted in the production of ω-hydroxy FA in an NADPH-dependent manner (Fig. 5*B*). The hydroxylation reactions by CYP generally require O_2 and NADPH. These results indicated that the substrates of CYP4F22 are indeed FAs.

Acylceramide specifically contains ULCFA (mostly C28–C36) as its FA component. It is possible that the substrate preference of CYP4F22 determines the FA chain length of acylceramides. To examine this possibility, we prepared HEK 293T cells producing different sets of ceramides with specific chain lengths by introducing particular combinations of ceramide synthase and FA elongase (ELOVL1 and CERS2, C22–C24 ceramides; ELOVL1 and CERS3, C26 ceramide; and ELOVL4 and CERS3, ≥C26 ceramides) (Fig. 5*C*) (28, 29). Mammals have six ceramide synthases (CERS1–6) and seven FA elongases (ELOVL1–7), and each exhibits characteristic substrate specificity (Fig. S2*B*) (2, 4, 5, 28). When CYP4F22 was expressed in these cells producing different ceramide species, ω-hydroxyceramides were produced in cells producing C26 ceramide (ELOVL1/CERS3 combination) and ≥C26 ceramides (the ELOVL4/CERS3 combination) but not in cells producing C22–C24 ceramides (the ELOVL1/CERS2 combination) (Fig. 5*D*). These results suggest that CYP4F22 can ω-hydroxylate ULCFAs (≥C26) but not VLCFAs (C22 and C24). The levels of ω-hydroxyceramide produced in ELOVL1/CERS3 cells were similar to those in ELOVL4/CERS3 cells, although the levels of nonhydroxyceramide substrates were much higher in ELOVL1/CERS3 cells (Fig. 5*C*). Thus, CYP4F22 exhibits especially high activity toward ULCFAs with ≥C28.

Discussion

Here we identified CYP4F22 as an ULCFA ω-hydroxylase involved in acylceramide production. Acylceramide is quite important for epidermal barrier formation, and impairment of its production (e.g. by *ELOVL4* and *CERS3* mutations) causes ichthyosis (15, 20). *CYP4F22* was first identified as an ARCI-causative gene by Fischer and her coworkers (21). They proposed that CYP4F22 and most other ichthyosis-causative genes are involved in a metabolic pathway producing 12-lipoxygenase products (hepoxilins and trioxilins) from arachidonic acid by analogy to the 5-lipoxygenase pathway creating leukotrienes. In their scenario, arachidonic acid is first converted to 12(*R*)-hydroperoxyeicosatetraenoic acid [12(*R*)-HPETE] by one of the ichthyosis gene products, ALOX12B, and then to 12(*R*)-hepoxilin A_3 by another ichthyosis gene product, ALOXE3. 12(*R*)-Hepoxilin A_3 is further converted to a triol compound, 12(*R*)-trioxilin A_3. CYP4F22 was proposed to be involved in the metabolism of 12(*R*)-trioxilin A_3 by converting 12(*R*)-trioxilin A_3 to 20-hydroxy-

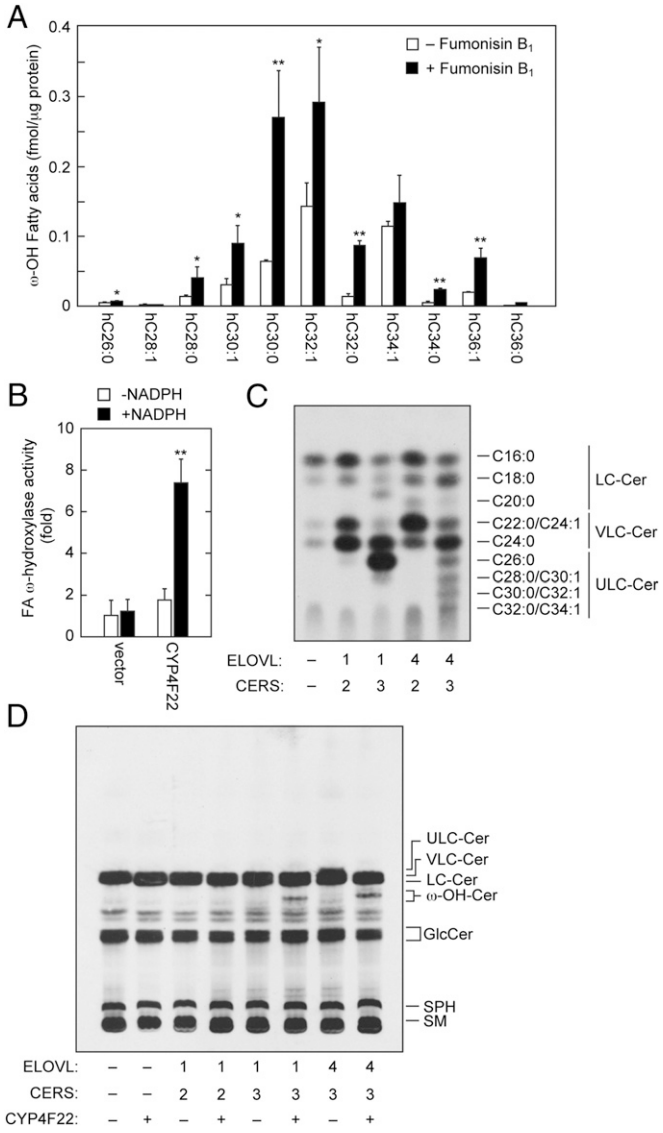

Fig. 5. CYP4F22 hydroxylates ULCFAs. (*A*) Keratinocytes were differentiated for 7 d in the presence or absence of 10 μM fumonisin B_1. Lipids were extracted, treated with an alkali, and derivatized to AMPP amides. Derivatized FAs were analyzed by a Xevo TQ-S LC/MS system and quantified by MassLynx software. Statistically significant differences are indicated; $*P < 0.05$, $**P < 0.01$; *t* test. hC26:0, hydroxy C26:0 FA. (*B*) Total membrane fractions (50 μg) prepared from BY4741 bearing the pAK1017 (vector) or pNS29 (*His_6-Myc-3xFLAG-CYP4F22*) plasmids were incubated with 10 μM C30:0 FA and 1 mM NADPH as indicated for 1 h at 37 °C. Lipids were extracted, derivatized to AMPP amides, and analyzed as in *A*. The values represent the amount of each FA ω-hydroxylase activity relative to that of the vector/−NADPH sample. The value of the CYP4F22/+NADPH sample was statistically different from the values of all other samples ($**P < 0.01$; *t* test). hC30:0, hydroxy C30:0 FA. (*C* and *D*) HEK 293T cells were transfected with the plasmids encoding *ELOVL1* or *ELOVL4*, *CERS2* or *CERS3*, and *CYP4F22*. Transfected cells were labeled with [^{3}H]sphingosine for 4 h at 37 °C. Extracted lipids were separated by reverse-phase TLC (*C*) or by normal-phase TLC (*D*) and detected by autoradiography. Cer, ceramide; GlcCer, glucosylceramide; SM, sphingomyelin; SPH, sphingosine; ω-OH, ω-hydroxy.

12(*R*)-trioxilin A_3. However, the exact roles of hepoxilins and trioxilins in epidermal barrier formation and/or keratinocyte differentiation are still unclear. Furthermore, recent findings have demonstrated that ALOX12B and ALOXE3 are involved in the reactions necessary for conversion of acylceramide to protein-bound ceramide, i.e., peroxidation of the linoleate moiety and subsequent epoxyalcohol derivatization (13). In addition, ALOX12B was proven not to be involved in hepoxilin/trioxilin production (30). These findings suggest that, although hepoxilin/trioxilin metabolism may not be relevant to the pathogenesis of ichthyosis, the impairment of acylceramide/protein-bound ceramide formation causes ichthyosis. Based on these recent findings, some researchers have predicted that CYP4F22 is involved in acylceramide generation (3, 31), but until now their suppositions have lacked experimental evidence.

We determined the membrane topology of CYP4F22 (Fig. 4*C*), which indicates that the large C-terminal hydrophilic domain including catalytic residues is located in the cytosol. Therefore, ω-hydroxylation of the ULCFA portion of acylceramide must occur on the cytosolic side of the ER membrane. Based on this finding, we propose a working model for the process of acylceramide production in the ER membrane as follows (Fig. S6). Elongation of palmitoyl-CoA to ULCFA-CoA occurs on the cytoplasmic side of the ER membrane. Because lipids comprising the ER membrane are mostly C16 and C18, ULCFA (C28–C36) portions of ULCFA-CoAs should be bent in the cytosolic leaflet of the ER membrane (Fig. S6) or should penetrate into the luminal leaflet. Although the latter possibility cannot be excluded, we prefer the former, because in the latter model ULCFA must flip-flop at least three times in the ER membrane in the course of acylceramide production. Because the substrates of CYP4F22 are ULCFAs (Fig. 5), ULCFA-CoAs should be converted to ULCFAs before ω-hydroxylation. After ω-hydroxylation of ULCFAs by CYP4F22, the resulting ω-hydroxy-ULCFA is converted to ω-hydroxy-ULCFA-CoA by acyl-CoA synthetase. ACSVL4/FATP4 is the candidate acyl-CoA synthetase for this reaction, because *Acsvl4*-mutant mice exhibited skin barrier defects (32). CERS3 catalyzes the formation of ω-hydroxyceramide from ω-hydroxy-ULCFA-CoA and LCB. An unknown acyltransferase then introduces linoleic acid into the ω-hydroxy group of ω-hydroxyceramide, generating acylceramide.

Our results presented here demonstrate, for the first time to our knowledge, that CYP4F22 is a bona fide ULCFA ω-hydroxylase required for acylceramide production. Our findings provide important insights into the molecular mechanisms of skin permeability barrier formation. Future development of compounds that strengthen the skin permeability barrier by increasing acylceramide-synthetic proteins such as ELOVL4, CERS3, and CYP4F22 may be useful for treatment of cutaneous disorders including ichthyosis and atopic dermatitis.

Materials and Methods

Details of the materials and methods used for all procedures are given in *SI Materials and Methods*.

Ethics. Stratum corneum was obtained from an ARCI patient (a 2-y-old girl) (25), carriers (her parents) (mother, 35 y old, c.1138delG; father, 39 y old, c.728G→A), and a healthy control (an 11-y-old girl). This study was approved by the ethical committees of Nagoya University Graduate School of Medicine and the Kao Corporation. Informed consent was obtained from all participants after the procedures had been explained. Informed consents for the girls were obtained from their parents.

Plasmids. Human *CYP4F* subfamily genes and the human *CERS3* gene were amplified by PCR using their respective forward and reverse primers listed in Table S2. The amplified DNAs first were cloned into pGEM-T Easy Vector (Promega) and then were transferred to the pCE-puro 3xFLAG-1 plasmid, a mammalian expression vector designed to produce an N-terminal 3xFLAG-tagged protein.

[^{3}H]Sphingosine Labeling Assay. Cells were labeled with 2 μCi [3-^{3}H]sphingosine (20 Ci/mmol; PerkinElmer Life Sciences) for 4 h at 37 °C. Lipids were extracted as described previously (28, 33) and separated by normal-phase TLC and reverse-phase TLC.

Lipid Analysis Using LC-MS. FAs and ceramides prepared from cultured cells were analyzed by reversed-phase LC/MS using ultra-performance liquid chromatography (UPLC) coupled with electrospray ionization (ESI) tandem triple quadrupole MS (Xevo TQ-S; Waters). Each ceramide species was detected by multiple reaction monitoring (MRM) by selecting the *m/z* ($[M–H_2O+H]^+$ and $[M+H]^+$) of specific ceramide species at Q1 and the *m/z* 264.2 at Q3 (Table S3). FAs were analyzed after derivatization to *N*-(4-aminomethylphenyl)pyridinium (AMPP) amides using the AMP^+ Mass Spectrometry Kit (Cayman Chemical). Hydroxy FA species were detected by MRM by selecting the *m/z* ($[M+H]^+$) of the derivatized hydroxy FA species at Q1 and the *m/z* 238.9 at Q3, corresponding to the fragment cleaved between C3 and C4 of derivatized FAs (Table S3). Stratum corneum ceramides were analyzed by reversed-phase LC/MS using the Agilent 1100 Series LC/MSD SL system (Agilent Technologies). Each ceramide species was detected by selected ion monitoring as *m/z* $[M+CH_3COO]^-$ (Table S4).

Immunoblotting. Immunoblotting was performed as described previously (34, 35) using anti-FLAG M2 (1.85 μg/mL) (Sigma), anti-calnexin 4F10 (1 μg/mL) (Medical & Biological Laboratories), or anti-GAPDH 6C5 (1 μg/mL; Ambion, Life Technologies) antibody as a primary antibody and an HRP-conjugated anti-mouse IgG $F(ab')_2$ fragment (1:7,500 dilution; GE Healthcare Life Sciences) as a secondary antibody. Labeling was detected using Pierce ECL Western Blotting Substrate (Thermo Fisher Scientific).

ACKNOWLEDGMENTS. This work was supported by the Creation of Innovation Centers for Advanced Interdisciplinary Research Areas Program from the Ministry of Education, Culture, Sports, Science and Technology of Japan (A.K.); and Grant-in-Aid for Scientific Research (A) 26251010 (to A.K.) and Grant-in-Aid for Young Scientists (A) 15H05589 (to Y.O.), both from the Japan Society for the Promotion of Science.

1. Uchida Y, Holleran WM (2008) Omega-O-acylceramide, a lipid essential for mammalian survival. *J Dermatol Sci* 51(2):77–87.
2. Mizutani Y, Mitsutake S, Tsuji K, Kihara A, Igarashi Y (2009) Ceramide biosynthesis in keratinocyte and its role in skin function. *Biochimie* 91(6):784–790.
3. Breiden B, Sandhoff K (2014) The role of sphingolipid metabolism in cutaneous permeability barrier formation. *Biochim Biophys Acta* 1841(3):441–452.
4. Kihara A (2012) Very long-chain fatty acids: Elongation, physiology and related disorders. *J Biochem* 152(5):387–395.
5. Sassa T, Kihara A (2014) Metabolism of very long-chain Fatty acids: Genes and pathophysiology. *Biomol Ther (Seoul)* 22(2):83–92.
6. Farwanah H, Wohlrab J, Neubert RH, Raith K (2005) Profiling of human stratum corneum ceramides by means of normal phase LC/APCI-MS. *Anal Bioanal Chem* 383(4): 632–637.
7. Masukawa Y, et al. (2008) Characterization of overall ceramide species in human *stratum corneum*. *J Lipid Res* 49(7):1466–1476.
8. Wertz PW, Cho ES, Downing DT (1983) Effect of essential fatty acid deficiency on the epidermal sphingolipids of the rat. *Biochim Biophys Acta* 753(3):350–355.
9. Imokawa G, et al. (1991) Decreased level of ceramides in stratum corneum of atopic dermatitis: An etiologic factor in atopic dry skin? *J Invest Dermatol* 96(4):523–526.
10. Ishikawa J, et al. (2010) Changes in the ceramide profile of atopic dermatitis patients. *J Invest Dermatol* 130(10):2511–2514.
11. Janssens M, et al. (2012) Increase in short-chain ceramides correlates with an altered lipid organization and decreased barrier function in atopic eczema patients. *J Lipid Res* 53(12):2755–2766.
12. Wertz PW, Downing DT (1987) Covalently bound ω-hydroxyacylsphingosine in the stratum corneum. *Biochim Biophys Acta* 917(1):108–111.
13. Zheng Y, et al. (2011) Lipoxygenases mediate the effect of essential fatty acid in skin barrier formation: A proposed role in releasing omega-hydroxyceramide for construction of the corneocyte lipid envelope. *J Biol Chem* 286(27):24046–24056.
14. Jobard F, et al. (2002) Lipoxygenase-3 (*ALOXE3*) and 12(*R*)-lipoxygenase (*ALOX12B*) are mutated in non-bullous congenital ichthyosiform erythroderma (NCIE) linked to chromosome 17p13.1. *Hum Mol Genet* 11(1):107–113.
15. Eckl KM, et al. (2013) Impaired epidermal ceramide synthesis causes autosomal recessive congenital ichthyosis and reveals the importance of ceramide acyl chain length. *J Invest Dermatol* 133(9):2202–2211.
16. Traupe H, Fischer J, Oji V (2014) Nonsyndromic types of ichthyoses - an update. *J Dtsch Dermatol Ges* 12(2):109–121.
17. Jennemann R, et al. (2012) Loss of ceramide synthase 3 causes lethal skin barrier disruption. *Hum Mol Genet* 21(3):586–608.
18. Krieg P, Fürstenberger G (2014) The role of lipoxygenases in epidermis. *Biochim Biophys Acta* 1841(3):390–400.
19. Akiyama M, Shimizu H (2008) An update on molecular aspects of the non-syndromic ichthyoses. *Exp Dermatol* 17(5):373–382.
20. Aldahmesh MA, et al. (2011) Recessive mutations in *ELOVL4* cause ichthyosis, intellectual disability, and spastic quadriplegia. *Am J Hum Genet* 89(6):745–750.
21. Lefèvre C, et al. (2006) Mutations in a new cytochrome P450 gene in lamellar ichthyosis type 3. *Hum Mol Genet* 15(5):767–776.
22. Behne M, et al. (2000) Omega-hydroxyceramides are required for corneocyte lipid envelope (CLE) formation and normal epidermal permeability barrier function. *J Invest Dermatol* 114(1):185–192.
23. Dhar M, Sepkovic DW, Hirani V, Magnusson RP, Lasker JM (2008) Omega oxidation of 3-hydroxy fatty acids by the human CYP4F gene subfamily enzyme CYP4F11. *J Lipid Res* 49(3):612–624.
24. Sanders RJ, Ofman R, Dacremont G, Wanders RJ, Kemp S (2008) Characterization of the human ω-oxidation pathway for ω-hydroxy-very-long-chain fatty acids. *FASEB J* 22(6):2064–2071.
25. Sugiura K, et al. (2013) Lamellar ichthyosis in a collodion baby caused by *CYP4F22* mutations in a non-consanguineous family outside the Mediterranean. *J Dermatol Sci* 72(2):193–195.
26. Szczesna-Skorupa E, Kemper B (1993) An N-terminal glycosylation signal on cytochrome P450 is restricted to the endoplasmic reticulum in a luminal orientation. *J Biol Chem* 268(3):1757–1762.
27. Shimozawa O, et al. (1993) Core glycosylation of cytochrome P-450(arom). Evidence for localization of N terminus of microsomal cytochrome P-450 in the lumen. *J Biol Chem* 268(28):21399–21402.
28. Ohno Y, et al. (2010) ELOVL1 production of C24 acyl-CoAs is linked to C24 sphingolipid synthesis. *Proc Natl Acad Sci USA* 107(43):18439–18444.
29. Sassa T, et al. (2013) Impaired epidermal permeability barrier in mice lacking *elovl1*, the gene responsible for very-long-chain fatty acid production. *Mol Cell Biol* 33(14): 2787–2796.
30. Krieg P, et al. (2013) *Aloxe3* knockout mice reveal a function of epidermal lipoxygenase-3 as hepoxilin synthase and its pivotal role in barrier formation. *J Invest Dermatol* 133(1):172–180.
31. Elias PM, et al. (2014) Formation and functions of the corneocyte lipid envelope (CLE). *Biochim Biophys Acta* 1841(3):314–318.
32. Moulson CL, et al. (2003) Cloning of wrinkle-free, a previously uncharacterized mouse mutation, reveals crucial roles for fatty acid transport protein 4 in skin and hair development. *Proc Natl Acad Sci USA* 100(9):5274–5279.
33. Nakahara K, et al. (2012) The Sjögren-Larsson syndrome gene encodes a hexadecenal dehydrogenase of the sphingosine 1-phosphate degradation pathway. *Mol Cell* 46(4): 461–471.
34. Kihara A, et al. (2003) Sphingosine-1-phosphate lyase is involved in the differentiation of F9 embryonal carcinoma cells to primitive endoderm. *J Biol Chem* 278(16): 14578–14585.
35. Kitamura T, Takagi S, Naganuma T, Kihara A (2015) Mouse aldehyde dehydrogenase ALDH3B2 is localized to lipid droplets via two C-terminal tryptophan residues and lipid modification. *Biochem J* 465(1):79–87.
36. Brachmann CB, et al. (1998) Designer deletion strains derived from *Saccharomyces cerevisiae* S288C: A useful set of strains and plasmids for PCR-mediated gene disruption and other applications. *Yeast* 14(2):115–132.
37. Kihara A, Sakuraba H, Ikeda M, Denpoh A, Igarashi Y (2008) Membrane topology and essential amino acid residues of Phs1, a 3-hydroxyacyl-CoA dehydratase involved in very long-chain fatty acid elongation. *J Biol Chem* 283(17):11199–11209.
38. Vasireddy V, et al. (2007) Loss of functional ELOVL4 depletes very long-chain fatty acids (≥C28) and the unique ω-O-acylceramides in skin leading to neonatal death. *Hum Mol Genet* 16(5):471–482.
39. Ogawa C, Kihara A, Gokoh M, Igarashi Y (2003) Identification and characterization of a novel human sphingosine-1-phosphate phosphohydrolase, hSPP2. *J Biol Chem* 278(2):1268–1272.
40. Kondo N, et al. (2014) Identification of the phytosphingosine metabolic pathway leading to odd-numbered fatty acids. *Nat Commun* 5:5338.